HAIBO WAN[1], BRUCE N. WILSON[2], DAVID R. SCHMIDT[2]

BIOFILTER MODEL DEVELOPMENT FOR THE REMOVAL OF POLLUTANTS FROM FEEDLOT RUNOFF

Biofilters are a potential treatment option for removing pollutants from feedlot runoff but little research has been done on their use and design. In this study, two mechanism-based models were developed to simulate biofilter processes: a first-order model and a logistic model. The two models were calibrated and evaluated using nitrogen (N) and phosphorus (P) data collected from rainfall events for an experimental biofilter at Melrose, Minnesota, USA. The first-order model predicted removal efficiencies better than the logistic model. The sensitivity analysis suggested that the predictions of the first-order model are more sensitive to parameter. In addition, the uncertainty analysis suggested that the range in predictive errors could be a consequence of uncertainty of estimating parameter from the limited data set for the first-order model. In contrast, the uncertainty analysis for the logistic model of N suggested that reasons other than the uncertainty in parameter estimation are needed to explain predictive errors. Overall, the study provides a useful tool for assessing biofilter performance that can easily be improved with larger observed data sets. The biofilter model has been implemented in the most recent version of the Minnesota feedlot annualized runoff model (MinnFARM).

1. INTRODUCTION

Runoff from animal feedlots can contribute to excessive nutrients in receiving waterbodies. Vegetative treatment systems (VTSs) are widely used in Minnesota and elsewhere to reduce feedlot runoff pollutants. These systems typically have a component of vegetative treatment area (VTA) designed to remove pollutants by infiltration. If designed and managed appropriately, VTAs are effective in feedlot runoff remediation [1]. The average removal rates of VTAs for both nitrogen (N) and phosphorus (P) can be as large as 70% [2, 3]. However, they can only be used at locations with adequate land area

_____

[1]Institute of Island and Coastal Ecosystems, Zhejiang University, Zhejiang, China, corresponding author, e-mail address: hwan@zju.edu.cn

[2]Department of Bioproducts and Biosystems Engineering, University of Minnesota, Minnesota, USA.

– the typical ratio for VTA area to feedlot area is 0.6 [4]. The VTAs also require mainte-
nance to have good vegetative growth during the life of the VTA, to minimize pollutant
accumulation by plant harvesting, to avoid channelization of flows within the VTA, and
must utilize pre-treatment systems such as settling basins [3]. Because of these limita-
tions, alternative treatment options are desired for feedlots.

Biofilters rely on microbial communities to remove contaminants from liquids.
These communities grow on moist surfaces of bioactive materials such as wood chips
or saw dusts. Biofilter medium supplies sufficient carbon for microbial growth. Micro-
organisms decompose carbon compounds using N and P in their surroundings [5].
Hence the concentrations of nutrients in feedlot runoff are well suited for direct treat-
ment by microbial growth. In addition, the consumption of nutrients by large numbers
of biofilter microorganisms could limit their availabilities to coliform bacteria (includ-
ing *Escherichia coli*) and thereby, potentially, reducing their levels in runoff. Biofilters
have been shown to be effective in removing contaminants in general but little research
has been done on their effectiveness to treat feedlot runoff [6–8]. Various engineering
aspects of biofiltration have been studied such as support media selection, bulk density,
moisture content, and C/N ratio [8, 9]. Widmer [8] has a good review of these features
as well as the microbial processes of biofiltration. However, more work is needed to
quantify the removal processes of contaminants in biofilters.

The goal of this study was to develop and evaluate predictive algorithms or models
for the removal of N and P in feedlot runoff by biofilters. A theoretical framework for
simulating a biofilter treatment system is first provided. This includes the use of a set-
tling chamber for pretreatment, similar to that used in VTSs. Two types of biofilter
models are then introduced: a first-order model and a logistic model. The next part of
the paper describes the sampling sites, experimental data used and the model evaluation
results. The two models are calibrated using N and P data collected at an experimental
biofilter from rainfall events. Sensitivity coefficients for both models are derived and
the uncertainty in model predictions is evaluated using a first-order analysis. The use-
fulness of the model to simulate the remediation of feedlot runoff by biofilter is then
discussed. In addition, these biofilter algorithms have been implemented, but not yet
released, in the widely used assessment tool in Minnesota called Minnesota feedlot an-
nualized runoff model (MinnFARM) [10, 11].

2. MODEL THEORY DEVELOPMENT

2.1. OVERVIEW

The Minnesota feedlot annualized runoff model (MinnFARM) was developed to
simulate the runoff and pollutant loading from feedlots and the removal of these pollu-
tants by VTSs and biofilters [10, 11]. Runoff from feedlot is based on the USDA-NRCS

curve number (CN) method [12]. Pollutant loadings for rainfall events at the feedlot edge are calculated using event mean concentrations that vary with animal management and season. Average annual loadings are computed using loadings corresponding to different events and weighting them by the likelihood of event occurrence. The runoffs and pollutant loadings at the outlet of feedlot are used as the inputs into the biofilter treatment system. Given the dynamic processes on the feedlot itself, considerable uncertainty exists in the MinnFARM predicted inflow characteristics into the biofilter model. A balanced approach is therefore taken in developing the biofilter algorithms. The model needs to have sufficient rigor to capture key components of filtration system but simple enough to represent processes by a reasonable number of parameters and at commensurate levels with the accuracy of inflow characteristics.
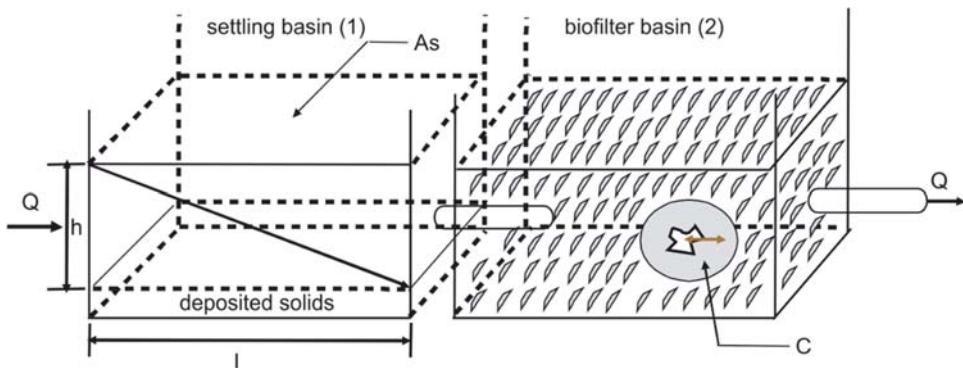

Fig. 1. Schematic of the biofilter treatment system

A schematic of a two-chamber biofilter treatment system is shown in Fig. 1. The first chamber is the settling basin that acts as a pretreatment for the removal of settleable solids, similar to that used in the VTSs, and the second chamber is the biofilter for the removal of contaminants by biochemical filtration. The first chamber is able to dampen the flow rate with its relatively large storage and restrictive pipe outlet, resulting in a more steady inflow rate into the biofilter. Separate algorithms are used and discussed for each of the chambers; however, the primary focus of this paper is the validity of the biochemical filtration of the second chamber. The brief description of the settling basin model is given to summarize the overall framework of the system.

2.2. CHAMBER 1. SETTLING BASIN

For the settling basin, the removal efficiency of settleable solids is determined by assuming constant flow rate for a "plug" moving between inlet and outlet, highly turbulent flows, a rectangular-shaped chamber with constant depth, no scour from the bottom, and uniform concentration at the inlet. The removal efficiency can then be computed as [13]

$$F_1 = 1 - \exp\left(\frac{\omega_s}{\omega_c}\right) = 1 - \exp\left(-\frac{\omega_s A}{Q}\right) \tag{1}$$

where F_1 is the removal efficiency, Q is the volumetric flow rate, A is the surface area of the settling basin, ω_s is the settling velocity of a particle of interest, and ω_c is the critical fall velocity. The average influent concentration is defined using the mass of contaminants divided by the runoff volume from the feedlot, as determined by the MinnFARM predictions. The effluent concentration is then obtained by the influent concentration multiplied by $1 - F_1$. The critical fall velocity corresponds to a particle that, under quiescent settling, would fall the entire flow depth within the detention time. The settling velocity in Eq. (1) is estimated using the Stokes equation developed for spherical particles with negligible inertia forces during settling. The Stokes equation can be written as follows [14]

$$\omega_s = \left(\frac{g}{18\mu}\right)(\rho_s - \rho_w) d^2 \tag{2}$$

where g is the acceleration of gravity, μ is the dynamic viscosity, ρ_s is the density of manure particles, ρ_w is the density of water, and d is the effective diameter of manure particles. Within MinnFARM, the dynamic viscosities are given in a look-up table that varies with runoff water temperatures from 0 to 40 °C. Densities of manure particles were taken for beef cattle, dairy cattle, chicken, horses, and swine [15]. For all breeds, manure particles are divided into three different size categories corresponding to representative diameters of 2000, 488 and 25 µm. The mass fraction of the manure for each of these categories is also determined [15].

2.3. CHAMBER 2. BIOFILTER BASIN

For the biofilter basin (Fig. 1), the removal of contaminants by settling is neglected. The concentration change over time is defined as

$$\frac{dC}{dt} = r \tag{3}$$

where r is the instantaneous removal rate of concentration. This equation allows the concentration of the constituent to be easily determined after it has moved through the biofilter. The removal efficiency for the biofilter (F_2) is determined as

$$F_2 = \frac{QC_0 - QC_f}{QC_0} = 1 - \frac{C_f}{C_0} \tag{4}$$

where C_0 is the influent concentration (corresponding to the effluent from settling chamber) and C_f is the concentration after a detention time exposure (T_d) to the biofilter.

Two different methods were explored to predict the removal rate. The simplest method assumes first-order processes [16]. For this method, r is defined as

$$r = -\kappa\,C \tag{5}$$

where κ is the decay coefficient (units $1/T$). This relationship is ideal for conditions when nutrient supply is unlimited and nearly optimal microbial growth. Concentration is then defined directly by substituting this relationship into Eq. (3) and by integrating between the limits of $t = 0$, $C = C_0$ and $t = T_d$, $C = C_f$, that is,

$$\frac{C_f}{C_0} = \exp\left(-\kappa T_d\right) \tag{6}$$

The removal efficiency for the first-order model is obtained directly from Eq. (6) as

$$F_2 = 1 - \exp\left(-\kappa T_d\right) \tag{7}$$

A different biofilter model can be developed using a logistic process. Here the rate of change in concentration is a function of the overall capacity for reduction. The logistic model can be written as [16]

$$r = -\kappa_l C\left(C - C_m\right) = \lambda C\left(1 - \frac{C}{C_m}\right) \tag{8}$$

where C_m is an equilibrium concentration at which the rate of removal is zero, λ is a rate coefficient (units $1/T$) defined as $\kappa_l C_m$. Conceptually, C_m is the concentration in the solution at which there is no potential gradient between the media and the solution. In contrast to the first-order model, the removal rate is limited by this equilibrium concentration.

The final concentration can be obtained for the logistic model by substituting its removal function r in Eq. (3). This relationship can then be integrated using partial fraction between $t = 0$, $C = C_0$ and $t = T_d$, $C = C_f$ as [16]

$$\frac{C_f}{C_0} = \frac{\exp\left(\lambda T_d\right)}{1 - \dfrac{C_0}{C_m}\left(1 - \exp\left(\lambda T_d\right)\right)} = \frac{\exp\left(\kappa_l C_m T_d\right)}{1 - \dfrac{C_0}{C_m}\left(1 - \exp\left(\kappa_l C_m T_d\right)\right)} \tag{9}$$

and therefore the corresponding removal efficiency is defined as

$$F_2 = 1 - \frac{\exp\left(\lambda T_d\right)}{1 - \dfrac{C_0}{C_m}\left(1 - \exp\left(\lambda T_d\right)\right)} = 1 - \frac{\exp\left(\kappa_l C_m T_d\right)}{1 - \dfrac{C_0}{C_m}\left(1 - \exp\left(\kappa_l C_m T_d\right)\right)} \tag{10}$$

2.4. HYDRAULIC VARIABLES

To simplify the analysis, steady flow for both chambers is assumed. The flow is defined in the MinnFARM algorithm using discharge through the outlet pipe for each of the chambers. A single, representative hydraulic head is used for each runoff event. Pipe flow is assumed and computed as [14]

$$Q_p = A \sqrt{\frac{2g(H + H')}{K_e + K_b + K_c L + 1}} \tag{11}$$

where Q_p is the pipe flow through the system, A is the cross-section area of pipe; g is the acceleration of gravity, H is head above the crest of the pipe's inlet, H' is the additional elevation corresponding to the difference between the inlet pipe crest and the outlet for no tailwater or an elevation for the adjustment of tailwater depth. The symbol L is the pipe length, K_e is the entrance-loss coefficient, K_b is the bend-loss coefficient, typical values for K_e and K_b are 1.0 and 0.5, respectively, and K_c is the friction-loss coefficient that can be computed from a known pipe diameter and Manning's roughness coefficient (n) [14].

Detention time is computed for pipe-flow conditions as [14]

$$T_d = \frac{V}{Q_p} \tag{12}$$

where V is the volume of water in the respective chamber for each rainfall event and Q is the outlet pipe flow as previously given by Eq. (11). Volume is computed as

$$V = lwh\varphi \tag{13}$$

where l, w, and h are the representative length, width, and depth of the water in the chamber and φ is the porosity of the biofilter.

3. DATA AND METHODS. MODEL EVALUATION

3.1. OVERVIEW

Since the theoretical framework for modeling the settling basin has been evaluated elsewhere [14, 17], model evaluation in this paper is focused on the removal within the biofilter. An important component of this evaluation is the assessment of model accuracy. Observed data of the removal efficiencies of biofilters of feedlot are limited. Additional insight into model calibration and validation is obtained by evaluating the sensitivity coefficients and model uncertainties.

3.2. EXPERIMENTAL SITE AND DATA COLLECTION

The experimental site for the observed data is located near Melrose, Minnesota, USA. The data were collected as part of grant activities supported by Minnesota Department of Agriculture and 319 EPA Funding [18]. This data set was independent of the modeling efforts. A schematic of the biofilter is shown in Fig. 2. The biofilter chamber had a length of 20.4 m and a width of 5.4 m. The depth of biofilter frame was around 0.85 m and the wood chips were piled to the rim. Pine bark-rich wood chips were used as the material for the biofilter. The porosity was estimated at 0.6 by the manager of the biofilter. Its outlet pipe had a length of 1.8 m, diameter of 0.1 m, and Manning's *n* of approximately 0.024.
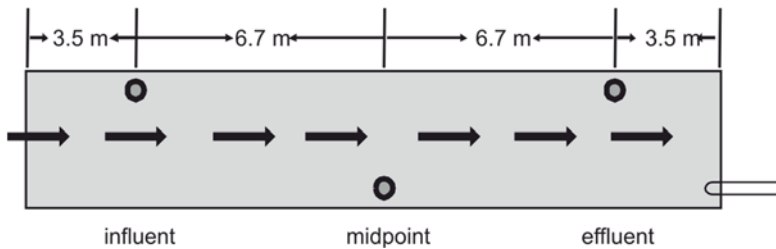

Fig. 2. Schematic of the biofilter at the evaluation site (modified from Fuchs, 2009)

Runoff was obtained from a feedlot with a surface area of approximately 0.4 ha. The ratio of the biofilter area to feedlot area is only 0.028, which is considerably smaller than a typical area ratio for VTAs of 0.6 [4]. The feedlot has a concrete surface and was used by approximately 156 dairy cows. Runoff from the feedlot was directed into a settling basin. The outflow from the settling basin was then diverted into the biofilter. Data were only collected in the biofilter itself. The evaluation of the model for the settling basin was therefore not possible with this data set.

Observed data were available for seven runoff events during an 18-month demonstration period from March 2008 to September 2009. The samples for nitrogen and phosphorus were taken once per event. The biofilter was uninstalled after this period because of the high maintenance cost. No other data from feedlot runoffs were available for use in this study.

Key characteristics of these events are summarized in Table 1. As shown in Fig. 2, water depths were monitored by ultrasonic sensors at three sample wells within the biofilter. The locations of these wells are labeled as circles. Water samples were collected from these three locations within the biofilter using ISCO samplers. Initial concentrations, C_0, were measured using samples collected at the left well. Final concentrations, C_f, were measured using samples collected at the right well except for the event of 14 March 2009 where the observed concentration was measured at the middle well. The collected samples were measured in the laboratory for TKN (total Kjeldahl nitrogen, measuring the total concentration of organic

nitrogen and ammonia) and TP (total phosphorus, measuring all the forms of phosphorus), using EPA 351.2 rev 2.0 and EPA 3653 methods, respectively.

Water depths D, concentrations C_0, C_f, and detention times T_d for the experimental sites

Date	D [m]	C_0 for N [mg·dm^{-3}]	C_f for N [mg·dm^{-3}]	C_0 for P [mg·dm^{-3}]	C_f for P [mg·dm^{-3}]	T_d [h]
9/15/2008	0.31	188	29.6	40.9	26.5	4.3
3/6/2009	0.51	705	198	25.2	7.1	5.5
3/14/2009	0.48	637	259[a]	28.7	20.6[a]	2.7
3/16/2009	0.39	454	321	39.8	12.2	4.8
4/3/2009	0.30	525	239	78.8	43.9	4.2
6/19/2009	0.24	367	134	81.3	28.7	3.8
9/10/2009	0.29	54.5	1.81	33.5	21.2	4.2

[a]C_f values for N and P on March 14, 2009 were measured at the middle point of the biofilter.

Detention time (T_d) is an important hydraulic characteristic of the biofilter and is also reported in Table 1. It was estimated from Eq. (12) for all of the observed events. The biofilter volume was determined using the surface area and the 24-h average depth at the middle well of the biofilter. The 24-h average depth at the middle well was used to determine the average flow depth h in the biofilter. Constant outflow rate was computed using the pipe flow relationship given by Eq. (11). The sum of K_e and K_b was set at 1.5 to account for energy losses at the pipe's inlet [14]. The friction loss coefficient, K_c, was calculated as 12.68 m^{-1} from Manning's n [14]. The value of H was set as 0.35 of the water depth. The value of H' was set as zero.

3.3. MODEL ACCURACY

The model accuracy was assessed by comparing the predicted and observed removal efficiencies. Observed removal efficiencies were computed directly from the observed data. The predicted removal efficiency for the first-order model was computed using Eq. (7) and for the logistic model using Eq. (10). Accuracy was assessed using the normalized mean square error (NMSE) [19]. A NMSE of zero corresponds to a perfect fit between predicted and observed values. A NMSE > 1 indicates that the observed data is better represented by the mean of the data than using the model predicted values.

3.4. SENSITIVITY ANALYSIS AND PARAMETER UNCERTAINTY

Sensitivity and model uncertainty analyses regarding parameters are used [20]. Sensitivity is defined as the change in the model outputs for a change in the parameter values and is therefore represented mathematically as [21]

$$S(\beta) = \frac{\partial \eta}{\partial \beta} \qquad (14)$$

where $S(\beta)$ is the sensitivity coefficient, η is the model predicted value, and β is the parameter of interest. For the first-order model of Eq. (7), the sensitivity coefficients of removal efficiency can be easily obtained with respect to the first-order coefficient as,

$$S(\kappa) = T_d \, \exp\left(-\kappa \, T_d\right) \qquad (15a)$$

For the logistic model of Eq. (10), the sensitivity coefficient of removal efficiency corresponding to κ_l is defined as

$$S\left(\kappa_l\right) = \frac{-C_m T_d \left(1 - \dfrac{C_0}{C_m}\right) \exp\left(\kappa_l C_m T_d\right)}{\left(1 - \dfrac{C_0}{C_m}\left(1 - \exp\left(\kappa_l C_m T_d\right)\right)\right)^2} \qquad (15b)$$

Relative sensitivity coefficients are often more useful in interpreting results. They are defined as [21]

$$S_r(\beta) = \frac{\dfrac{\partial \eta}{\eta}}{\dfrac{\partial \beta}{\beta}} \qquad (16)$$

The relative sensitivity coefficients for the first-order model and the logistic model are defined directly from Eqs. (7) and (10) as

$$S_r(\kappa) = \kappa T_d \exp \frac{\left(-\kappa T_d\right)}{F_2} \qquad (17a)$$

$$S_r(\kappa_l) = \frac{-\kappa_l C_m T_d \left(1 - \dfrac{C_0}{C_m}\right) \exp(\kappa_l C_m T_d)}{F_2 \left(1 - \dfrac{C_0}{C_m}\left(1 - \exp\left(\kappa_l C_m T_d\right)\right)\right)^2} \qquad (17b)$$

The sensitivity coefficients and relative sensitivity coefficients are not constant due to varying inflow conditions, detention times, and biofilter properties. They provide

fundamental information about the two models and specific values will be given for the conditions of the experimental site in the Results and Discussion section. Sensitivity coefficients also are important in determining the uncertainty in predicted response using a first-order analysis. With the first-order analysis, the predicted response function is linearized by using a Taylor series expansion with neglected second and higher order terms. The variance of the predicted value is then defined as [22]

$$\text{Var}(\eta) = \sum_{j=1}^{n} \sum_{i=1}^{n} S(\beta_j) S(\beta_i) \text{Cov}(\beta_i, \beta_j) \tag{18a}$$

where Var(η) is the variance of prediction, $S(\beta_i)$ and $S(\beta_j)$ are the sensitivity coefficients for the ith and jth parameters, and Cov(β_i, β_j) is the covariance between β_i and β_j. For the special case of parameters that are independent, the first-order variance of predicted response is defined as

$$\text{Var}(\eta) = \sum_{i=1}^{n} S(\beta_i)^2 \text{Var}(\beta_i) \tag{18b}$$

where Var(β_i) is the variance of the parameter β_i and $Var(\eta)$ is a measure of uncertainty in prediction. Therefore for the special case of a single input parameter of the decay coefficient, the variance of the prediction is simply estimated as the product of squared equations 15a or 15b and the variance of the decay coefficient.

4. RESULTS AND DISCUSSION

4.1. PARAMETERS ESTIMATION

First-order decay coefficient κ. The decay coefficient κ of the first-order model was computed directly for each event from Eq. (6) using measured influent (C_0) and effluent (C_f) concentrations and estimated detention time. Decay coefficients for N and P for the seven rainfall events are given in Table 2.

Relationships between first-order model decay coefficient κ and possible independent variables of cumulative temperature, precipitation depth, average flow depth, and detention time were investigated using regression techniques. Cumulative temperature is defined as the sum of average daily air temperature greater than 0 °C since the start of the year, which is a surrogate for the cumulative microbial growth. The only significant predictor variable was found to be cumulative temperature for N. Trends with cumulative temperature are shown in Fig. 3, where linear regression indicates better fit than non-linear. The discussion as follows is limited to linear relationship only. The

coefficient of determination is 0.65 (compared to that of less than 0.1 for either precipitation, average flow depth or detention time) and the linearity is significant with a *p*-value less than 0.05.

Estimated decay coefficients for individual events

Date	First-order coefficient κ [h^{-1}]		Logistic coefficient κ_l [dm^{-3}·h^{-1}·mg^{-1}]	
	N	P	N	P
9/15/2008	0.43	0.1	0.0068	0.0032
3/6/2009	0.23	0.23	0.0007	0.02
3/14/2009	0.33	0.12	0.0009	0.0053
3/16/2009	0.07	0.25	0.0002	0.0125
4/3/2009	0.19	0.14	0.0006	0.0025
6/19/2009	0.27	0.27	0.0013	0.0061
9/10/2009	0.81	0.11	0.1881	0.0043
Mean	0.33	0.17	0.0018 (0.0284)[a]	0.0077
Variance	0.057	0.005	6.25×10^{-6} (4.97×10^{-3})[a]	4.03×10^{-5}

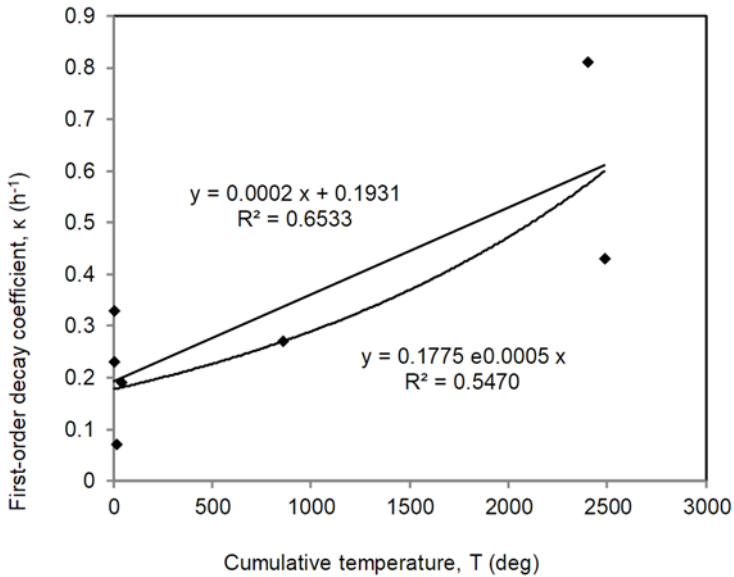[a]The parentheses include the likely outlier of September 10, 2009.

Fig. 3. Trend of the first-order decay coefficient
of N with cumulative temperature

A larger data set is obviously needed before more definitive statements can be made about the effectiveness of the regression equation. It is, however, rational to expect a microbial population increase with cumulative temperature and a corresponding increase in κ. No significant predictor variable was found for the P first-order model (coefficient of determination is less than 0.3 for all of the four variables). Significant regression results are summarized in Table 3.

<div align="right">T a b l e 3</div>

Significant regression relationships for the first-order and logistic coefficients

Coefficient	T or D range	Relationship	R^2	p-value	MSE
κ for N		$\kappa = 0.0002T + 0.1931$[a]	0.65	<0.05	0.024
κ for P	0–25 °C	$\kappa = -3\times10^{-5}T + 0.201$[a]	0.27	>0.1	4.67×10^{-3}
κ_l for N		$\kappa_l = 2.43\times10^{-6}T + 0.0004$[a]	0.94	<0.01	4.74×10^{-7}
κ_l for P	0.2–0.5 m	$\kappa_l = 0.0425D - 0.0077$[b]	0.47	0.09	2.59×10^{-5}

[a]T denotes cumulative temperature – the sum of average daily air temperature higher than 0 °C since the start of the year.
[b]D denotes average flow depth.

Equilibrium concentration C_m. Attempts to estimate logistic-model parameters of κ_l and C_m were initially done by trying to calibrate both of them. Pairs of values were carefully selected. The optimal set of parameters was evaluated by using the minimal sum of squares of the difference between predicted and observed removal efficiencies. This approach resulted in an estimate of C_m that was physically unrealistic. Thereafter C_m was set at 1 mg·dm^{-3} for both N and P – this value was less than the minimum observed concentrations of N and P at the biofilter outlet. Physically, the value of C_m is likely a function of time. For the removal of phosphorus of enhanced sand filtration, Erickson et al. [23] found C_m varied by the relationship of:

$$C_m = C_{in} \left(1 - \beta_0 e^{-\beta_1 \sum m}\right) \tag{19}$$

where C_{in} is the influent concentration, $\sum M$ is the instantaneous sum of phosphorus mass retained, β_0 and β_1 are two rate coefficients. Because of the limited data available, C_m is a constant in this study.

Logistic Decay coefficient κ_l. For a specified C_m, only κ_l or λ needs to be estimated from the observed data. Values of κ_l are selected for the study. For the specified C_m values and for the detention times given in Table 1, the decay coefficient κ_l was computed directly from measured influent and effluent concentrations using Eq. (9). The results for N and P are also given in Table 2 for each observed event. The mean and variance for the estimated κ_l

values for N were calculated with and without the event of 10 September 2009, respectively. Values that included this likely outlier are given in parentheses.
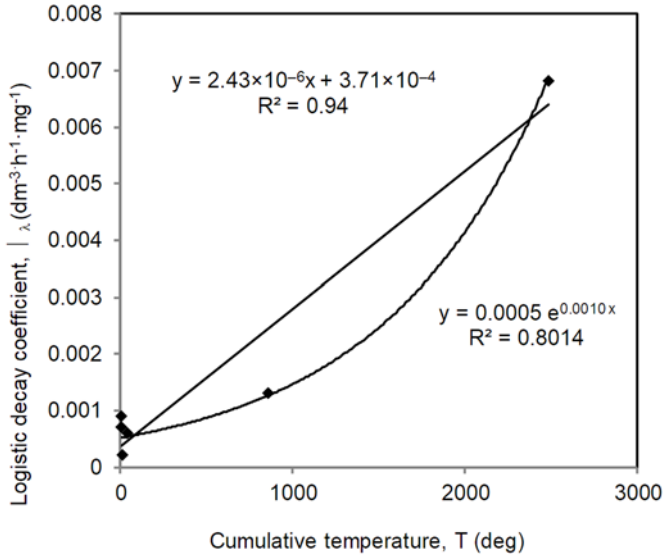

Fig. 4. Trend of the logistic decay coefficient of N with cumulative temperature (with the event of September 10, 2009 removed as outlier)
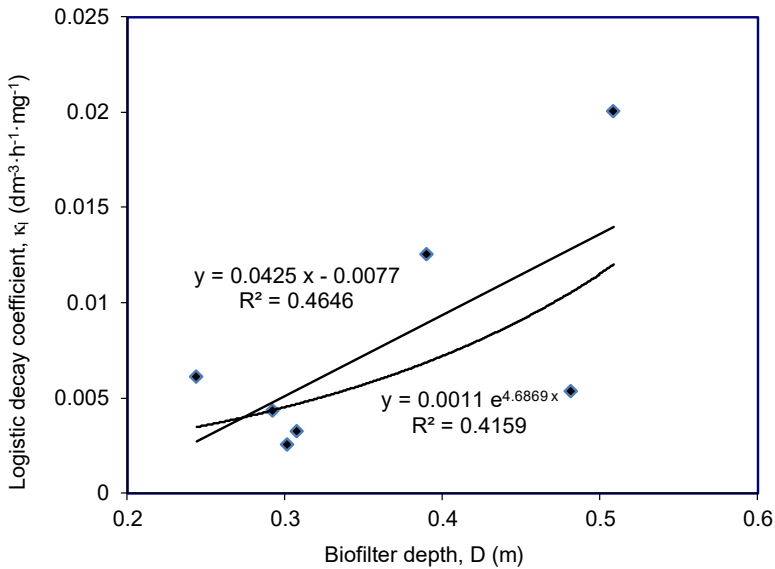

Fig. 5. Trend of the logistic decay coefficient of P on the average flow depth

Trends in κ_l as a function of independent variables of cumulative temperature, precipitation depth, average flow depth, and detention time were also explored using regression techniques. Linear regression indicates better fit than non-linear one for both N and P. The discussion as follows is limited to linear relationships only. With the removal of the apparent outlier for the event of 10 September 2009 (at which the κ_l value 0.1881 is more than 100 times larger than the κ_l from any other event), the significant predictor variable was found to be cumulative temperature for N. The coefficient of determination is 0.94 for N and the linearity is significant with a *p*-value less than 0.01 (Fig. 4). For P, average flow depth and detention time are significant predictor variables, with the coefficients of determination of 0.47 and 0.45, respectively. The average flow depth is the strongest predictor with a *p*-value of 0.09. Trends in κ_l with the average flow depth are shown in Fig. 5. Only one predictor of average flow depth was selected for the logistic model of P in order to avoid overfitting. Significant regression results are summarized in Table 3.

4.2. MODEL ACCURACY

N model. For this study, the predicted values were computed using estimates of the first-order and logistic coefficients obtained from regression relationships of Table 3 and as well by using the average values. Observed and predicted removal efficiencies for N are shown in Table 4.

Table 4

Accuracy of the removal efficiency (dimensionless)
for N using first-order and logistic models

Date	Observed value	Using regression		Using averages	
		First-order	Logistic	First-order	Logistic
9/15/2008	0.84	0.93	0.84	0.76	0.59
3/6/2009	0.72	0.66	0.60	0.84	0.87
3/14/2009 (mid)	0.59	0.41	0.40	0.59	0.76
3/16/2009	0.29	0.61	0.47	0.79	0.80
4/3/2009	0.54	0.57	0.51	0.75	0.80
6/19/2009	0.63	0.72	0.77	0.71	0.71
9/10/2009	0.97	0.92	0.58	0.75	0.29
NMSE		0.55	0.88	1.30	3.15

Both κ and κ_l values for N were determined by their regression relationships with cumulative temperature. For N, using the regression estimate of κ, the NMSE for the first-order model was 0.55; and using that of κ_l, the corresponding NMSE of the logistic model was 0.88. Also shown in Table 4 are the predicted removal efficiencies calculated using the average κ and κ_l as given in Table 2. For N, the NMSEs are 1.30 and 3.15 for

the first-order and logistic models, respectively. Not surprisingly, the observed removal efficiencies are predicted more accurately using coefficients estimated from regression relationships than using average values. The first-order model more accurately predicted observed removal efficiencies than the logistic model.

P model. Observed and predicted removal efficiencies for P are shown in Table 5. Since no significant regression relationship could be established for the first-order model, only the coefficients for the logistic model were represented by the corresponding regression result (of average flow depth) in Table 3. The predicted removal efficiencies for both the first-order and logistic models were estimated using the average values of κ and κ_l in Table 2. For these averages, the NMSEs for the first-order and logistic models are 0.6 and 1.06, respectively. The first-order model therefore represented the observed removal efficiencies more accurately than the logistic model. The regression estimates of the κ_l for the logistic model resulted in a substantial improvement in the prediction accuracy: The NMSE using the regression estimates reduced NMSE from 1.06 to 0.75.

Table 5

Accuracy of the removal efficiency (dimensionless)
for P using first-order and logistic models

Date	Observed value	Using regression		Using averages	
		First-order	Logistic	First-order	Logistic
9/15/2008	0.35	N/A	0.48	0.52	0.57
3/6/2009	0.72	N/A	0.64	0.61	0.50
3/14/2009 (mid)	0.28	N/A	0.48	0.37	0.36
3/16/2009	0.69	N/A	0.62	0.56	0.58
4/3/2009	0.44	N/A	0.62	0.51	0.71
6/19/2009	0.65	N/A	0.43	0.48	0.70
9/10/2009	0.37	N/A	0.38	0.51	0.51
NMSE		N/A	0.75	0.60	1.06

4.3. MODEL SENSITIVITY AND UNCERTAINTY

Relative sensitivities. They were calculated using Eqs. (17a) and (17b). The averages and ranges of relative sensitivity coefficients among the seven events for N and P are reported in Table 6. The model sensitivity to its parameters should ideally be equal to the actual sensitivity of the biofilter's removal efficiencies to its media characteristics. Using regression relationship for N, a 1% change in κ corresponds to an approximate 0.57% change in the predicted removal efficiency for the first-order model; whereas for the logistic model, a 1% change in κ_l corresponds to an approximate change of 0.39%

in predicted removal efficiency. Using average values for N, a 1% change in κ corresponds to an approximate 0.59% change in the predicted removal efficiency for the first-order model; whereas for the logistic model, a 1% change in κ_l corresponds to an approximate change of 0.31% in predicted removal efficiency. Using average values for P, a 1% change in κ corresponds to an approximate 0.77% change in the predicted removal efficiency for the first-order model; whereas for the logistic model, a 1% change in κ_l corresponds to an approximate change of 0.52% in predicted removal efficiency. For both N and P, the first-order model is more sensitive to κ than the logistic model is to κ_l.

Table 6

Relative sensitivities S_r (dimensionless) for N and P

Model		S_r(N)		S_r(P)	
		First-order (κ)	Logistic (κ_l)	First-order (κ)	Logistic (κ_l)
Regression	Mean	0.57	0.39	N/A	0.26
	Range	(0.21, 1.27)	(0.16, 0.86)	N/A	(0.13, 0.52)
Average	Mean	0.59	0.31	0.77	0.52
	Range	(0.36, 1.11)	(0.16, 0.57)	(0.51, 1.05)	(0.32, 0.82)

For N, relative sensitivities for the first-order models are similar for coefficients estimated using regression relationships and those using average values, relative sensitivities for the logistic models are higher for coefficients estimated using regression relationships than those using average values. For P, relative sensitivities for the logistic models are lower for coefficients estimated using regression relationships than those using average values. For N and P combined, the relative sensitivities did not show clear pattern in terms of the distinction between coefficients estimated using regression relationships and those using average values. It is easy to understand that the relative sensitivities of coefficients do not depend on specified data used for calculation, but the mechanism of models.

Model uncertainty. The first-order variances of predicted values are calculated using Eq. (18b) for the seven events. Their mean values are then computed using the geometric mean, because of the large range in variance of prediction. Results are given in Table 7 for N and P. The variances of κ and κ_l corresponding to average-estimated coefficients are estimated using their variance in the seven events. The variances of κ and κ_l using regression relationships are estimated using the MSEs in Table 3 (except κ for P, where regression relationship is not available). Uncertainties in the slope and intercept values were therefore not included in these estimates. To illustrate key concepts, and because of limited data set for regression analysis, discussion will focus on the results obtained corresponding to average-estimated coefficients. For N, standard deviations of uncertainty are $SD(\eta_{N,1}) = 0.24$, $SD(\eta_{N,L}) = 0.25$ for the first-order and logistic

models, respectively; whereas the standard deviations of uncertainty are $SD(\eta_{P,1}) = 0.14$ and $SD(\eta_{P,L}) = 0.19$ for predicted P values for the first-order and logistic models, respectively. For both N and P, to some degree the first-order model has lower model uncertainty than the logistic model.

Table 7

Variances of predictions (dimensionless) for N and P

Model		N Var(η_N)		P Var(η_P)	
		First-order (κ)	Logistic (κ_l)	First-order (κ)	Logistic (κ_l)
Regression	Mean[a]	0.025	0.016	N/A	0.0002
	Range	(0.002, 0.086)	(0.0002, 0.1845)	N/A	(0.00005, 0.0005)
Average	Mean[a]	0.059	0.064	0.02	0.036
	Range	(0.044, 0.069)	(0.025, 0.120)	(0.014, 0.022)	(0.027, 0.041)

[a]Geometric mean.

Moreover, of particular interest in this study is determining whether the difference between predicted and observed removal efficiencies given in Tables 4 and 5 can be attributed to uncertainty in the estimate of κ for the first-order model or κ_l for the logistic model. For many probability density functions, the probability is small for a difference value greater than two standard deviations of uncertainty. For N with exclusion of the likely outlier of 16 March 2009, for all seven events the differences between the observed and predicted N removal efficiencies for the first-order model (see Table 4) using averages are within one $SD(\eta_i)$. Differences between observed and predicted values could thus be a consequence of the uncertainty in estimating κ. However for the logistic model, four out of seven differences for using average are greater than or equal to one $SD(\eta_{N,L})$, with two differences larger than two $SD(\eta_{N,L})$. Differences here are more likely a consequence of not adequately representing processes with the logistic model and therefore not in the uncertainty in estimating κ_l.

For P, the first-order model and the logistic model have similar performance in representing the processes by the decay parameter. For the first-order model using the average parameter, two differences are larger than and one difference is equal to one $SD(\eta_{P,l})$. For the logistic model using the average parameter, three differences are larger than one $SD(\eta_{P,L})$. No difference is larger than two $SD(\eta_{P,l})$ or $SD(\eta_{P,L})$. For both models, differences between observed and predicted values could mostly attribute to the uncertainty in estimating decay parameter. However, to point it out here, $SD(\eta_{P,l})$ has a value substantially lower than that of $SD(\eta_{P,L})$.

In general, the first-order models had better prediction accuracy than the logistic models for both N and P. The first-order models are therefore better suited to represent the N and P removal processes. The superior performance of first-order model can be attributed to: (1) N and P supplies from feedlot runoff were sufficient during runoff

events, which satisfied the condition for first-order model; (2) logistic model had a C_m coefficient, little information was available to estimate this parameter. Logistic model might be more useful if C_m is investigated with carefully designed experiments in the future. In addition, the first-order model is more sensitive to κ than the logistic model is to κ_l for both N and P, likely because the logistic model represented the process less well as the first-order model.

It is not surprising that the removal efficiencies varied greatly between sampling events. Collecting data under field conditions for complex runoff events is challenging. Many factors can impact contaminant removal processes, such as pH and concentration of inhibiting materials in the biofilter. More carefully designed experiments are needed to fully explore these factors. The results of these experiments are anticipated to be easily incorporated into the biofilter models proposed in this study.

5. CONCLUSIONS

The first-order model better represented biofilter processes than the logistic model. Firstly, the first-order model predicted removal efficiencies with greater accuracy than the logistic model. The NMSEs were always smaller for the first-order model using estimated coefficients of either regression relationships (if a regression relationship is available) or averages for both nitrogen (N) and phosphorous (P). Second, the uncertainty analysis for the logistic model of N suggested that reasons other than the uncertainty in estimating the decay coefficient are needed to explain the predictive errors. In contrast, predictive errors are within the reasonable range corresponding to the uncertainty in estimating the decay coefficients of first-order model for both N and P, which suggested that the first-order model is adequate. Thirdly, the predicted values of first-order model are more sensitive to its decay coefficient than the logistic model.

More data are needed to better define the decay coefficients and to evaluate the model performance. Additional data would also be helpful in evaluating the effectiveness of models to represent different design dimensions and alternative biofilter media. Nonetheless, the analytical work has provided a useful theoretical foundation for further modeling exploration and can ultimately be helpful in establishing engineering standards.

SYMBOLS

F_1 – removal efficiency of the settling basin
Q – volumetric flow rate, $m^3 \cdot s^{-1}$
A – surface area of the settling basin, or cross-section area of a pipe, m^2
ω_s – settling velocity of a fluid particle, $m \cdot s^{-1}$
ω_c – critical fall velocity, $m \cdot s^{-1}$
g – acceleration of gravity, 9.8 $m \cdot s^{-2}$
μ – dynamic viscosity of a fluid, $kg \cdot s^{-1} \cdot m^{-1}$

ρ_s – density of manure particles, kg·m^{-3}
ρ_w – density of water, kg·m^{-3}
d – effective diameter of manure particles, μm
F_2 – removal efficiency of the biofilter
C_0 – influent concentration, mg·dm^{-3}
C_f – effluent concentration, mg·dm^{-3}
T_d – detention time, h
κ – first-order decay coefficient, h^{-1}
κ_l – logistic decay coefficient, dm^{-3}·h^{-1}·mg^{-1}
C_m – equilibrium concentration at which the rate of removal is zero, mg·dm^{-3}
Q_p – pipe flow rate, m^3·s^{-1}
L – pipe length, m
H – head above the crest of the pipe's inlet, m
H' – additional head to H, m
K_e – entrance-loss coefficient, dimensionless
K_b – bend-loss coefficient, dimensionless
K_c – friction-loss coefficient, m^{-1}
n – Manning's roughness coefficient, s·m$^{-1/3}$
V – water volume in the chamber, m^3
l, w, h – length, width, and depth of the chamber, m
φ – porosity of the biofilter, dimensionless fraction
NMSE – normalized mean square error, dimensionless
β – decay parameter, κ or κ_l
$S(\beta)$ – sensitivity coefficient of β
$S_r(\beta)$ – relative sensitivity coefficient of β, dimensionless
η – model prediction of F_2, dimensionless fraction
Var(η) – variance of model prediction η, dimensionless
SD(η) – standard deviation of model prediction η, dimensionless

ACKNOWLEDGMENTS

REFERENCES

[1] *Vegetated Treatment Systems for Open Lot Runoff. A Collaborative Report*, R. Koelsch, B. Kintzer, D. Meyer (Eds.), U.S. Department of Agriculture, Natural Resources Conservation Service, 2006, http://www.heartlandwq.iastate.edu/ManureManagement/AlternativeTech/Avtsguidance/, accessed 10 April 2016.
[2] IKENBERRY C.D., MANKIN K.R., *Review of Vegetative Filter Strip Performance for Animal Waste Treatment*, ASAE Paper No. MC00128, ASAE, St. Joseph, MI, USA, 2000.
[3] KOELSCH R.K., LORIMOR J.C., MANKIN K.P., *Vegetative treatment systems for management of open lot runoff. Review of literature*, Appl. Eng. Agric., 2006, 22 (1), 141.
[4] *NRCS-Minnesota, Conservation Practice Standard 635. Vegetated Treatment Area, Minnesota Department of Agriculture*, St. Paul, MN, USA, 2009, https://efotg.sc.egov.usda.gov/references/public /MN /Archived_635mn_160307.pdf, accessed 10 April 2016.

[5] BRADY N.C., WEIL R.R., *The Nature and Properties of Soils*, 13th Ed., Pearson Prentice Hall, Upper Saddle River, NJ, USA, 2002, 498–542.

[6] U.S. Forest Service, *A cheaper way to clean water*, NewsLine, 2002, 1 (2), 1, http://www.fpl.fs.fed.us /documnts/newsline/newsline-2002-2.pdf, accessed 10 April 2016.

[7] ROBERTSON W.D., FORD G.I., LOMBARDO P.S., *Wood-based filter for nitrate removal in septic systems*, T. ASAE, 2005, 48 (1), 121.

[8] WIDMER S.P., *Remediation of Nitrogen, Phosphorus and E. coli from Feedlot Runoff Using Different Biofilter Media*, MS thesis, University of Minnesota, Department of Soil, Water and Climate, St. Paul, MN, USA, 2007.

[9] *On-Farm Composting Handbook*, R. Rynk (Ed.), NRAES-54, Northeast Regional Agricultural Engineering Service, Ithaca, NY, USA, 1992.

[10] SCHMIDT D., WILSON B.N., *Minnesota Feedlot Annualized Runoff Model (MinnFARM)*, Technical Documentation, University of Minnesota, St. Paul, MN, USA, 2007.

[11] SCHMIDT D., WILSON B.N., *Minnesota Feedlot Annualized Runoff Model (MinnFARM) version 2.1 User Guide*, University of Minnesota, St. Paul, MN, USA, 2008, http://www1.extension.umn.edu /agriculture/manure-management-and-air-quality/feedlots-and-manure-storage/docs/minnfarm-users-guide.pdf, accessed 10 April 2016.

[12] USDA-SCS, *Section 4. Hydrology*, [in:] *Soil Conservation Service National Engineering Handbook*, U.S. Department of Agriculture, Soil Conservation Service, Washington, D.C., USA, 1985.

[13] CORDOBA-MOLINA J.F., HUDGINS R.R., SILVESTON P.L., *Settling in continuous sedimentation tanks*, J. Environ. Eng. Div., Am. Soc. Civ. Eng., 1978, 104, 1263.

[14] HAAN C.T., BARFIELD B.J., HAYES J.C., *Design Hydrology and Sedimentology for Small Catchments*, Academic Press, San Diego, CA, USA, 1994.

[15] HAFEZ A.A.R., AZEVEDO J., RUBIN J., STOUT P.R., *Physical Properties of Farm Animal Manure*, California Agricultural Experimental Station Bulletin 867, University of California, Davis, CA, USA, 1974.

[16] SHULER M.L., KARGI F., *Bioprocess Engineering. Basic Concepts*, Prentice Hall PTR, Englewood Cliffs, NJ, USA, 1992.

[17] WILSON B.N., BARFIELD B.J., *Modeling sediment detention ponds using reactor theory and advection-diffusion concepts*, Water Resour. Res., 1985, 21 (4), 523.

[18] Fuchs D.J., *Feedlot Runoff Pollution Removal by Organic Biofilter Demonstration*, Final Report of EPA 319 Demonstration, Education and Research Project, MPCA Contract A91219, Stearns County Soil and Water Conservation District, Waite Park, MN, USA, 2009.

[19] GERSHENFELD N.A., WEIGEND A.S., *The Future of Time Series: Learning and Understanding*, [in:] A.S. Weigend, N.A. Gershenfeld (Eds.), *Time Series Prediction: Forecasting the Future and Understanding the Past*, SFI Studies in the Sciences of Complexity, Proc. Vol. 15, Addison-Wesley, Boston, MA, USA, 1993.

[20] WILSON B.N., NIEBER J.L., *As simple as possible: status and need in hydrological and water quality modeling*, paper presented at Urban Runoff Modeling: Intelligent Modeling to Improve Stormwater Management Conference, Humboldt State University, Archata, CA, USA, 22–27 July 2007.

[21] JAMES L.D., BURGES S.J., *Selection, Calibration and Testing of Hydrologic Models*, [in:] C.T. Haan, H.P. Johnson, D.L. Brakensiek (Eds.), *Hydrologic Modeling of Small Watersheds*, ASAE Monograph No. 5, ASAE, St. Joseph, MI, USA, 1982.

[22] GAREN D.C., BURGES S.J., *Approximate error bounds for simulated hydrograph*, J. Hydraul. Div., Am. Soc. Civ. Eng., 1981, 107 (HY11), 1519.

[23] ERICKSON A.J., GULLIVER J.S., WEISS P.T., *Enhanced sand filtration for storm water phosphorus removal*, J. Environ. Eng., 2007, 133 (5), 485.